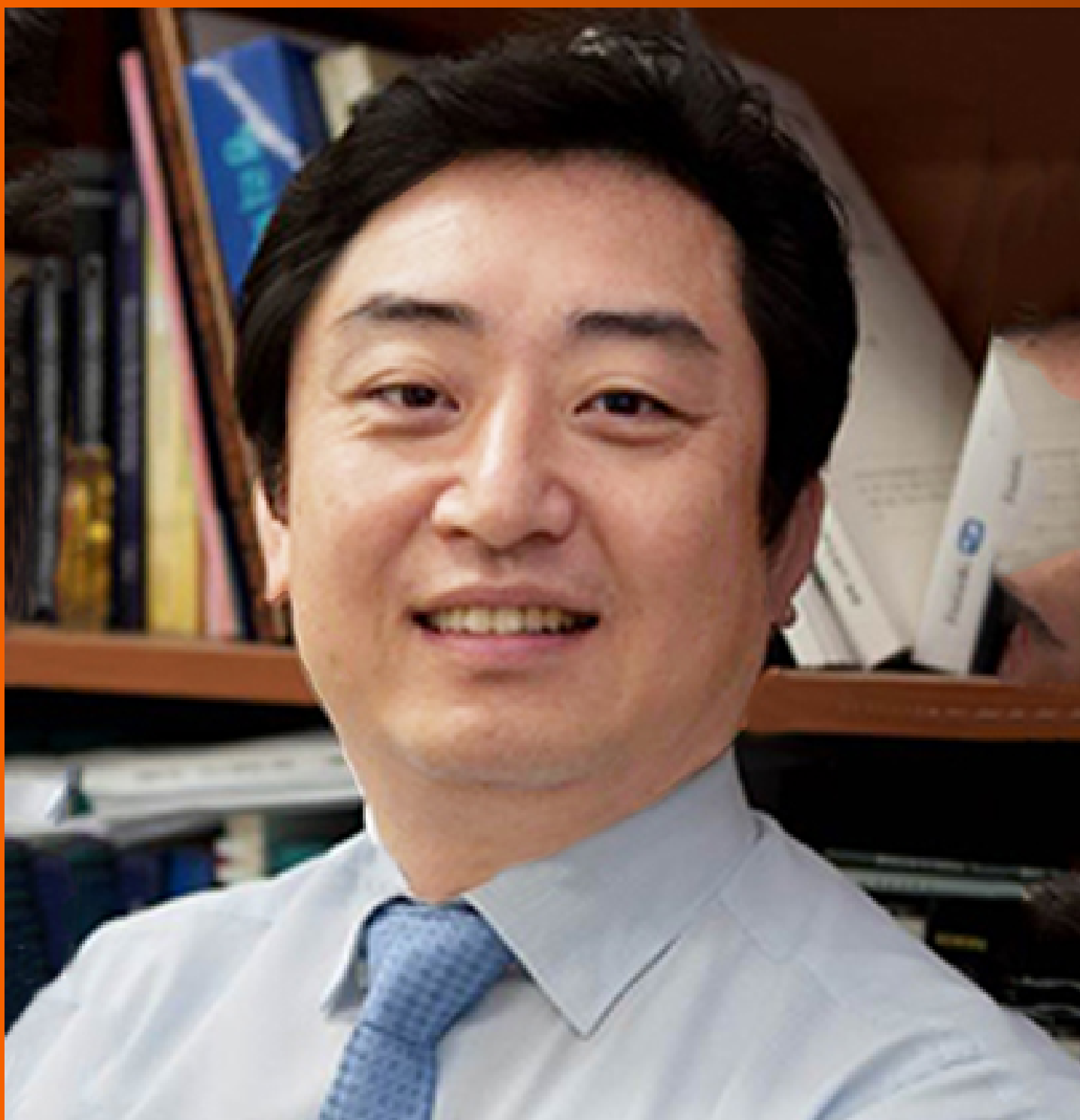


World Journal of *Gastroenterology*

World J Gastroenterol 2020 March 21; 26(11): 1107-1230



**OPINION REVIEW**

- 1107** Current status of endoscopic sleeve gastropasty: An opinion review
Wang JW, Chen CY

REVIEW

- 1113** Circulating microRNAs as non-invasive biomarkers for hepatitis B virus liver fibrosis
Iacob DG, Rosca A, Ruta SM

MINIREVIEWS

- 1128** Similarities and differences in guidelines for the management of pancreatic cysts
Lanke G, Lee JH

ORIGINAL ARTICLE**Basic Study**

- 1142** Effect of prolonged omeprazole administration on segmental intestinal Mg^{2+} absorption in male Sprague-Dawley rats
Suksridechacin N, Kulwong P, Chamniansawat S, Thongon N
- 1156** Protective effects of panax notoginseng saponin on dextran sulfate sodium-induced colitis in rats through phosphoinositide-3-kinase protein kinase B signaling pathway inhibition
Lu QG, Zeng L, Li XH, Liu Y, Du XF, Bai GM, Yan X

Retrospective Cohort Study

- 1172** Non-robotic minimally invasive gastrectomy as an independent risk factor for postoperative intra-abdominal infectious complications: A single-center, retrospective and propensity score-matched analysis
Shibasaki S, Suda K, Nakauchi M, Nakamura K, Kikuchi K, Inaba K, Uyama I
- 1185** Preoperative albumin levels predict prolonged postoperative ileus in gastrointestinal surgery
Liang WQ, Zhang KC, Li H, Cui JX, Xi HQ, Li JY, Cai AZ, Liu YH, Zhang W, Zhang L, Wei B, Chen L

Retrospective Study

- 1197** Landscape of BRIP1 molecular lesions in gastrointestinal cancers from published genomic studies
Voutsadakis IA
- 1208** Radiomics model based on preoperative gadoteric acid-enhanced MRI for predicting liver failure
Zhu WS, Shi SY, Yang ZH, Song C, Shen J

Observational Study

- 1221** Subtle skills: Using objective structured clinical examinations to assess gastroenterology fellow performance in system based practice milestones

Papademetriou M, Perrault G, Pitman M, Gillespie C, Zabar S, Weinshel E, Williams R

ABOUT COVER

Associate Editor of *World Journal of Gastroenterology*, Suk Woo Nam, PhD,
Professor, Department of Pathology, The Catholic University of Korea,
College of Medicine, Seoul 137-701, South Korea

AIMS AND SCOPE

The primary aim of *World Journal of Gastroenterology* (WJG, *World J Gastroenterol*) is to provide scholars and readers from various fields of gastroenterology and hepatology with a platform to publish high-quality basic and clinical research articles and communicate their research findings online.

WJG mainly publishes articles reporting research results and findings obtained in the field of gastroenterology and hepatology and covering a wide range of topics including gastroenterology, hepatology, gastrointestinal endoscopy, gastrointestinal surgery, gastrointestinal oncology, and pediatric gastroenterology.

INDEXING/ABSTRACTING

The WJG is now indexed in Current Contents®/Clinical Medicine, Science Citation Index Expanded (also known as SciSearch®), Journal Citation Reports®, Index Medicus, MEDLINE, PubMed, PubMed Central, and Scopus. The 2019 edition of Journal Citation Report® cites the 2018 impact factor for WJG as 3.411 (5-year impact factor: 3.579), ranking WJG as 35th among 84 journals in gastroenterology and hepatology (quartile in category Q2). CiteScore (2018): 3.43.

RESPONSIBLE EDITORS FOR THIS ISSUE

Responsible Electronic Editor: *Yu-Jie Ma*
Proofing Production Department Director: *Xiang Li*

NAME OF JOURNAL

World Journal of Gastroenterology

ISSN

ISSN 1007-9327 (print) ISSN 2219-2840 (online)

LAUNCH DATE

October 1, 1995

FREQUENCY

Weekly

EDITORS-IN-CHIEF

Subrata Ghosh, Andrzej S Tarnawski

EDITORIAL BOARD MEMBERS

<http://www.wjgnet.com/1007-9327/editorialboard.htm>

EDITORIAL OFFICE

Ze-Mao Gong, Director

PUBLICATION DATE

March 21, 2020

COPYRIGHT

© 2020 Baishideng Publishing Group Inc

INSTRUCTIONS TO AUTHORS

<https://www.wjgnet.com/bpg/gerinfo/204>

GUIDELINES FOR ETHICS DOCUMENTS

<https://www.wjgnet.com/bpg/GerInfo/287>

GUIDELINES FOR NON-NATIVE SPEAKERS OF ENGLISH

<https://www.wjgnet.com/bpg/gerinfo/240>

PUBLICATION MISCONDUCT

<https://www.wjgnet.com/bpg/gerinfo/208>

ARTICLE PROCESSING CHARGE

<https://www.wjgnet.com/bpg/gerinfo/242>

STEPS FOR SUBMITTING MANUSCRIPTS

<https://www.wjgnet.com/bpg/GerInfo/239>

ONLINE SUBMISSION

<https://www.f6publishing.com>



Retrospective Study

Radiomics model based on preoperative gadoteric acid-enhanced MRI for predicting liver failure

Wang-Shu Zhu, Si-Ya Shi, Ze-Hong Yang, Chao Song, Jun Shen

ORCID number: Wang-Shu Zhu (0000-0002-9739-0767); Si-Ya Shi (0000-0002-1416-9128); Ze-Hong Yang (0000-0001-7562-3710); Chao Song (0000-0002-3538-381X); Jun Shen (0000-0001-7746-5285).

Author contributions: Zhu WS and Shi SY contributed equally to this work; Zhu W, Shi S, and Shen J designed the research; Zhu W and Shi S collected and analyzed the data, and wrote the manuscript; Yang Z and Song C analyzed and interpreted the data; Shen J wrote and revised the manuscript; All co-authors participated in writing and checking the manuscript, and approved the submitted manuscript.

Supported by the Guangdong Province Universities and Colleges Pearl River Scholar Funded Scheme (2017); and the Guangdong Natural Science Foundation, No. 2017A030313777.

Institutional review board

statement: This study was reviewed and approved by the Ethics Committee of Sun Yat-Sen Memorial Hospital.

Informed consent statement:

Patients were not required to give informed consent to the study because the analysis used anonymous clinical data that were obtained after each patient agreed to treatment by written consent.

Conflict-of-interest statement: The authors declare no conflict of interest.

Data sharing statement: No additional data are available.

Wang-Shu Zhu, Si-Ya Shi, Ze-Hong Yang, Chao Song, Jun Shen, Department of Radiology, Sun Yat-Sen Memorial Hospital, Sun Yat-Sen University, Guangzhou 510120, Guangdong Province, China

Wang-Shu Zhu, Si-Ya Shi, Ze-Hong Yang, Chao Song, Jun Shen, Guangdong Provincial Key Laboratory of Malignant Tumor Epigenetics and Gene Regulation, Medical Research Center, Sun Yat-Sen Memorial Hospital, Sun Yat-Sen University, Guangzhou 510120, Guangdong Province, China

Corresponding author: Jun Shen, MD, Department of Radiology, Sun Yat-Sen Memorial Hospital, Sun Yat-Sen University, No. 107 Yanjiang Road West, Guangzhou 51012, Guangdong Province, China. shenjun@mail.sysu.edu.cn

Abstract

BACKGROUND

Postoperative liver failure is the most severe complication in cirrhotic patients with hepatocellular carcinoma (HCC) after major hepatectomy. Current available clinical indexes predicting postoperative residual liver function are not sufficiently accurate.

AIM

To determine a radiomics model based on preoperative gadoteric acid-enhanced magnetic resonance imaging for predicting liver failure in cirrhotic patients with HCC after major hepatectomy.

METHODS

For this retrospective study, a radiomics-based model was developed based on preoperative hepatobiliary phase gadoteric acid-enhanced magnetic resonance images in 101 patients with HCC between June 2012 and June 2018. Sixty-one radiomic features were extracted from hepatobiliary phase images and selected by the least absolute shrinkage and selection operator method to construct a radiomics signature. A clinical prediction model, and radiomics-based model incorporating significant clinical indexes and radiomics signature were built using multivariable logistic regression analysis. The integrated radiomics-based model was presented as a radiomics nomogram. The performances of clinical prediction model, radiomics signature, and radiomics-based model for predicting post-operative liver failure were determined using receiver operating characteristics curve, calibration curve, and decision curve analyses.

RESULTS

Open-Access: This article is an open-access article that was selected by an in-house editor and fully peer-reviewed by external reviewers. It is distributed in accordance with the Creative Commons Attribution NonCommercial (CC BY-NC 4.0) license, which permits others to distribute, remix, adapt, build upon this work non-commercially, and license their derivative works on different terms, provided the original work is properly cited and the use is non-commercial. See: <http://creativecommons.org/licenses/by-nc/4.0/>

Manuscript source: Unsolicited manuscript

Received: October 12, 2019

Peer-review started: October 12, 2019

First decision: January 13, 2020

Revised: February 18, 2020

Accepted: February 21, 2020

Article in press: February 21, 2020

Published online: March 21, 2020

P-Reviewer: Tsoulfas G

S-Editor: Ma YJ

L-Editor: Filipodia

E-Editor: Liu JH



Five radiomics features from hepatobiliary phase images were selected to construct the radiomics signature. The clinical prediction model, radiomics signature, and radiomics-based model incorporating indocyanine green clearance rate at 15 min and radiomics signature showed favorable performance for predicting postoperative liver failure (area under the curve: 0.809-0.894). The radiomics-based model achieved the highest performance for predicting liver failure (area under the curve: 0.894; 95%CI: 0.823-0.964). The integrated discrimination improvement analysis showed a significant improvement in the accuracy of liver failure prediction when radiomics signature was added to the clinical prediction model (integrated discrimination improvement = 0.117, $P = 0.002$). The calibration curve and an insignificant Hosmer-Lemeshow test statistic ($P = 0.841$) demonstrated good calibration of the radiomics-based model. The decision curve analysis showed that patients would benefit more from a radiomics-based prediction model than from a clinical prediction model and radiomics signature alone.

CONCLUSION

A radiomics-based model of preoperative gadoxetic acid-enhanced MRI can be used to predict liver failure in cirrhotic patients with HCC after major hepatectomy.

Key words: Liver failure; Radiomics; Gadoxetic acid; Magnetic resonance imaging; Hepatocellular carcinoma

©The Author(s) 2020. Published by Baishideng Publishing Group Inc. All rights reserved.

Core tip: Serological indexes, indocyanine green clearance rate at 15 min, liver volumetry, and clinical scoring systems are commonly used to determine liver function capacity and predict postoperative residual liver function. However, these indexes are not sufficiently accurate for predicting the risk of postoperative liver failure. We constructed a radiomics signature based on preoperative hepatobiliary phase gadoxetic acid-enhanced magnetic resonance imaging. This radiomics signature achieves favorable performance in predicting liver failure in cirrhotic patients with hepatocellular carcinoma after major hepatectomy. Incorporating indocyanine green clearance rate at 15 min into the radiomics signature further improves the predictive performance for postoperative liver failure.

Citation: Zhu WS, Shi SY, Yang ZH, Song C, Shen J. Radiomics model based on preoperative gadoxetic acid-enhanced MRI for predicting liver failure. *World J Gastroenterol* 2020; 26(11): 1208-1220

URL: <https://www.wjgnet.com/1007-9327/full/v26/i11/1208.htm>

DOI: <https://dx.doi.org/10.3748/wjg.v26.i11.1208>

INTRODUCTION

Postoperative liver failure is the most serious complication for patients with hepatocellular carcinoma (HCC) after major hepatectomy, and it is caused by insufficient function of the remnant liver. Liver failure not only influences the physical state of patients and contributes to cancer recurrence, but also prolongs hospital stay, thereby increasing overall medical costs^[1]. Therefore, preoperative liver function prediction is highly important for risk stratification in patients considering major hepatectomy. To date, liver function assessment primarily relies on the serological indexes, indocyanine green (ICG) retention rate at 15 min (ICG-R15)^[2], liver volumetry based on computed tomography (CT)^[3], and clinical scoring systems^[4,5]. Unfortunately, these measures for predicting the prognosis of postoperative residual liver function after hepatectomy are not sufficiently accurate^[6].

Gadoxetic acid-enhanced magnetic resonance imaging (MRI) has been widely used to distinguish benign and malignant liver lesions^[7]. As gadoxetic acid can be selectively absorbed by functional hepatocytes, signal intensity of liver measured on preoperative gadoxetic acid-enhanced hepatobiliary phase (HBP) images has also

been applied to assess liver function^[8,9]. However, parenchymal damage is often not homogeneously distributed in the liver^[10,11] and liver abnormalities are frequently and increasingly heterogeneous during the development of cirrhosis^[8]. The measurement of mean signal intensity in a predefined larger area of liver parenchyma is insensitive for identifying regional variations, thereby omitting heterogeneity that is informative for liver damage in cirrhotic patients.

Radiomics is a method utilizing high-dimensional data mined from digital medical images for quantitative measurement, and can be applied to improve predictive, diagnostic, and prognostic accuracy to support clinical decision^[12,13]. Previously, radiomics approaches based on MRI or CT images have been extensively applied for differential diagnosis, monitoring of disease progression, and evaluation of the treatment response^[14,15]. However, whether a radiomics-based model based on gadoxetic acid-enhanced MRI can be used for predicting liver failure in cirrhotic patients with HCC after major hepatectomy has not been determined so far.

In this study, we investigated the value of a radiomics model based on gadoxetic acid-enhanced MRI for predicting liver failure after major hepatectomy in cirrhotic patients with HCC.

MATERIALS AND METHODS

Study population

This retrospective study was approved by the Institutional Review Board of Sun Yat-Sen Memorial Hospital of Sun Yat-Sen University, and written informed consent was waived by the institutional review board. Patients with HCC who had major liver resection between June 2012 and June 2018 were identified from the institutional HCC database. Patients were enrolled in this study if they had: (1) Serologically-proven hepatitis B-related cirrhosis; (2) HCC confirmed by surgical pathology; (3) Undergone major liver resection; and (4) Undergone preoperative gadoxetic acid-enhanced MRI within 7 d before liver surgery. A total of 619 patients met this inclusion criteria. Patients were excluded if they had an unresectable tumor and previously received treatment, such as chemotherapy or transarterial chemoembolization ($n = 173$), had minor liver resection (< 3 Couinaud liver segments) ($n = 322$), or had artifacts on their HBP MRI ($n = 13$). Finally, 101 patients were included in this study (Figure 1). Postoperative liver failure was identified according to the method proposed by Amber *et al*^[16], which defines liver failure as the presence of the following: encephalopathy with hyperbilirubinemia, total bilirubin > 4.1 mg/dL without an obstruction or bile leak, international normalized ratio of prothrombin time > 2.5 , and ascites (drainage > 500 mL/d). All patients had undergone the ICG test within 7 d before surgery, as previously described^[17]. The preoperative serum levels of alanine aminotransferase, aspartate aminotransferase, total bilirubin, albumin, alkaline phosphatase, platelet, prothrombin time, prealbumin, and cholinesterase, Child-Pugh classification, and the degree of liver fibrosis were retrieved from the hospital medical records. The liver fibrosis was detected by Masson staining of the resected liver specimens and graded according to a previously reported method^[18].

Clinical prediction model construction

The normality of distribution of clinical variables was assessed by the Shapiro-Wilk test. Continuous variables were presented as median \pm range and compared using the unpaired *t*-test, two-tailed *t*-test, or Mann-Whitney test. Categorical variables were presented as number (percentage), and compared using Mann-Whitney test. Univariable logistic regression analysis was used to determine clinical variables associated with liver failure. Those significant variables were chosen for multivariable binary logistic regression analysis using the forward likelihood ratio selection method to determine the independent risk factors for liver failure. The independent risk factors were used to construct a clinical prediction model.

MRI

MRI was performed on a 3.0 Tesla clinical scanner (Achieva TX; Philips Healthcare, Best, The Netherlands) with a 16-channel sense torso coil. The imaging sequences included axial fat-suppressed T2-weighted imaging [repetition time/echo time (TR/TE), 1650/80 ms; slice thickness/gap, 3.5/1 mm; matrix, 528 \times 288; number of signals acquired (NSA), 2], axial T1-weighted imaging using mDixon fast field echo sequence (number of echoes, 2; TR, 3.4 ms; TE, 1.14 and 2.1 ms; flip angle, 10°; slice thickness/gap, 3/1 mm; matrix, 528 \times 288; NSA, 1) and coronal T1 high resolution isotropic volume examination (THRIVE) sequence (TR/TE, 3.1/1.4 ms; flip angle, 10°; slice thickness/gap, 3/1 mm; matrix, 528 \times 288; NSA, 2). After intravenous injection of

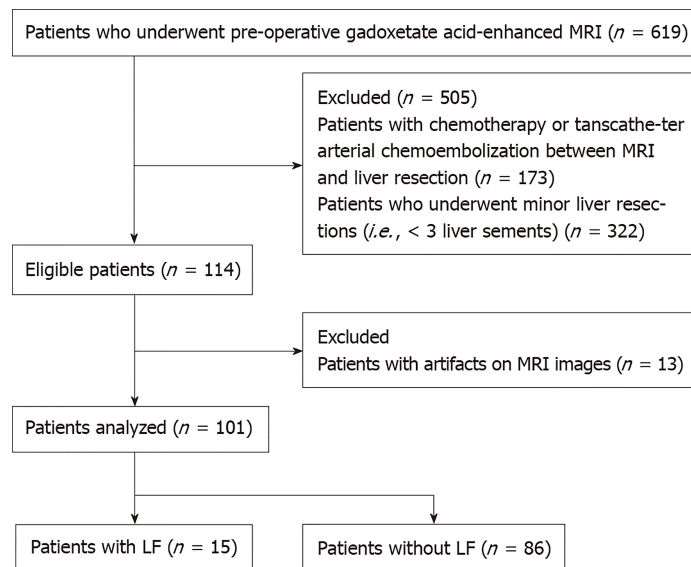


Figure 1 Flow diagram shows patient selection. LF: Liver failure; MRI: Magnetic resonance imaging.

gadoteric acid (Gd-EOB-DTPA; Primovist, Bayer-Schering Pharma, Berlin, Germany) at a dosage of 0.025 mmol/kg of body weight *via* the antecubital vein at a rate of 2.5 mL/s, patients underwent multiphasic axial contrast-enhanced T1 high resolution isotropic volume examination (e-THRIVE) imaging, which was performed with the same parameters as their unenhanced counterparts. Early arterial phase, later arterial phase, portal phase, venous phase, and equilibrium phase images were obtained respectively at 20, 30, 40, 60 and 100 s after the injection of contrast agents. The HBP images were obtained at 20 min after the injection of gadoteric acid.

Radiomic feature selection and radiomics signature construction

The flow diagram of radiomic feature selection and radiomics signature construction is shown in [Figure 2](#). Region of interests (ROIs) for the liver were drawn along the margin of the entire liver parenchyma on HBP images, by excluding hepatic masses, large hepatic vessels, and bile ducts on HBP images. The ROI was further refined to exclude areas of fat, air, and bone using a thresholding procedure (Centricity PACS 4.0, GE Medical Systems). Then the processed HBP images were transferred to an off-line workstation and analyzed by a quantitative analysis software (Omni Kinetics, GE Healthcare). Radiomic features were analyzed by two radiologists (Z.W. and Y.Z. with 3 and 13 years of experience in diagnostic imaging respectively) in a blinded manner independently. For radiomic features, 61 descriptors including the first-order and distribution statistics (23 descriptors) to reflect basic characters of image uniformity, gray-level co-occurrence matrix (28 descriptors) to describe the homogeneity, and gray-level run length matrix (10 descriptors) to indicate image coarseness were obtained. The categories of the radiomic features are listed in [Table 1](#) in detail. Intra- and inter-observer reproducibility of radiomic feature extraction was determined by the intraclass correlation coefficients (ICCs). The result from two readers were averaged for analysis. To assess intra-observer reproducibility, HBP images from 24 randomly selected patients were chosen for ROI segmentation and feature extraction analysis by reader 1 (Z.W.). After 1 wk, reader 1 repeated the same procedure. An ICC value > 0.75 represents good to excellent agreement, and the value between 0.4 and 0.75 indicates moderate agreement.

The least absolute contraction selection operator (LASSO) logistic regression was used to select radiomic features with non-zero coefficients^[19]. The multivariable logistic regression with enter method was used to construct radiomics signature. The radiomics score (Rad-score) were calculated *via* a linear combination of selected features that were weighted by their respective coefficients.

Development and performance of radiomics-based prediction model

To develop an integrated radiomics-based prediction model, the independent predictors of clinical variables and radiomics signature were chosen for multivariable logistic regression analysis to determine the parameters that can best predict the risk of liver failure. A collinearity diagnosis was made on the logistic regression model to test the independence of predictors. The established radiomics-based model was presented as a radiomics nomogram. The prediction performance of this radiomics

Table 1 Categories of the quantitative radiomics features obtained for analysis

Groups	Detailed parameters
First-order and distribution statistics, $n = 23$	Minimum intensity, Maximum intensity, Mean intensity, Median intensity, Standard deviation, Variance, Volume count, Voxel value sum, Range mean deviation, Relative deviation, Skewness, Kurtosis, Uniformity, Energy, Entropy, Frequency size, Quantile 5, Quantile 10, Quantile 25, Quantile 50, Quantile 75, Quantile 90, Quantile 95
Gray-level co-occurrence matrix, $n = 28$	Glcmm bin size, Glcmm total frequency, Glcmm matrix mean, Glcmm relative Frequency, Energy, Entropy, Inertia, Correlation, Inverse difference moment, Cluster shade, Cluster prominence, Haralick correlation, Haralick entropy, Angular second moment, Contrast, Haralick variance, sum Average, sum Variance, sum Entropy, Difference variance, Difference entropy, Inverse difference moment normalized, Minimum intensity, Maximum intensity, Number of intensity bins, Minimum size, Maximum size, Number of size bins
Gray-level run length matrix, $n = 10$	Short run emphasis (SRE), Long run emphasis (LRE), Gray level non-uniformity (GLN), Run length non-uniformity (RLN), Low gray level run emphasis (LGLRE), High gray level run emphasis (HGLRE), Short run low gray level emphasis (SRLGLE), Short run high gray level emphasis (SRHGLE), Long run low gray level emphasis (LRLGLE), Long run high gray level emphasis (LRHGLE)

nomogram was measured by correcting 1000 bootstrap samples to reduce the overfit bias. The calibration of the nomogram was evaluated using a calibration curve. The goodness-of-fit of the nomogram was assessed by the Hosmer-Lemeshow test.

Statistical analysis

The performance of the clinical prediction model, radiomics signature and radiomics-based model for predicting liver failure was determined using the receiver operating characteristic curve analysis. The discrimination performance was quantified using the calculation of the area under the curve (AUC) and its 95% confidence intervals (CIs). The sensitivity, specificity, positive predicted value (PPV), negative predicted value and accuracy of the models were also calculated. The integrated discrimination improvement (IDI) and continuous net reclassification improvement indexes were used to assess the additional predictive value. The net benefits for a range of threshold probabilities by the decision curve analysis was calculated to estimate the clinical utility of the clinical prediction model, radiomics signature and radiomics-based model. Statistical tests were performed using software SPSS version 21.0 (SPSS, Chicago, Ill, United States), R version 3.3.3 (R Development Core Team, Vienna, Austria) and MedCalc Statistical Software version 17.1 (MedCalc Software, Ostend, Belgium). A two sided P value < 0.05 was considered to indicate a statistically significant difference.

RESULTS

Patient characteristics and clinical prediction model

Among the 101 patients included, there were 88 men (age range, 27-78 years; median age, 55 years), and 13 women (age range, 22-66 years; median age, 53 years). Fifteen patients had liver failure after major hepatectomy, and the remaining 86 patients did not have liver failure. Among 15 patients with liver failure, 3 of them had a sustained type of liver failure and died, while 12 of them developed liver failure immediately after surgery and recovered after proper treatment. The clinicopathologic characteristics of the enrolled patients are shown in Table 2. There were no differences in the sex, age, liver fibrosis, or Child-Pugh classifications between patients with or without liver failure ($P > 0.05$). The aspartate aminotransferase level, alkaline phosphatase (ALP) level and ICG-R15 were significantly different between two groups ($P = 0.030$, 0.004 , and 0.002 , respectively). Univariable and multivariable logistic analysis showed that the ALP level and ICG-R15 were independent risk factors for liver failure ($P < 0.05$). Thus, the ALP level and ICG-R15 were selected to build the clinical prediction model and the radiomics-based model.

Radiomic feature selection and radiomics signature construction

The intra-observer ICCs (ranging from 0.780 to 0.992) and the inter-observer ICCs (ranging from 0.763 to 0.935) suggested good intra- and inter-observer reproducibility for feature extraction analysis. Among 61 radiomic features, five features were

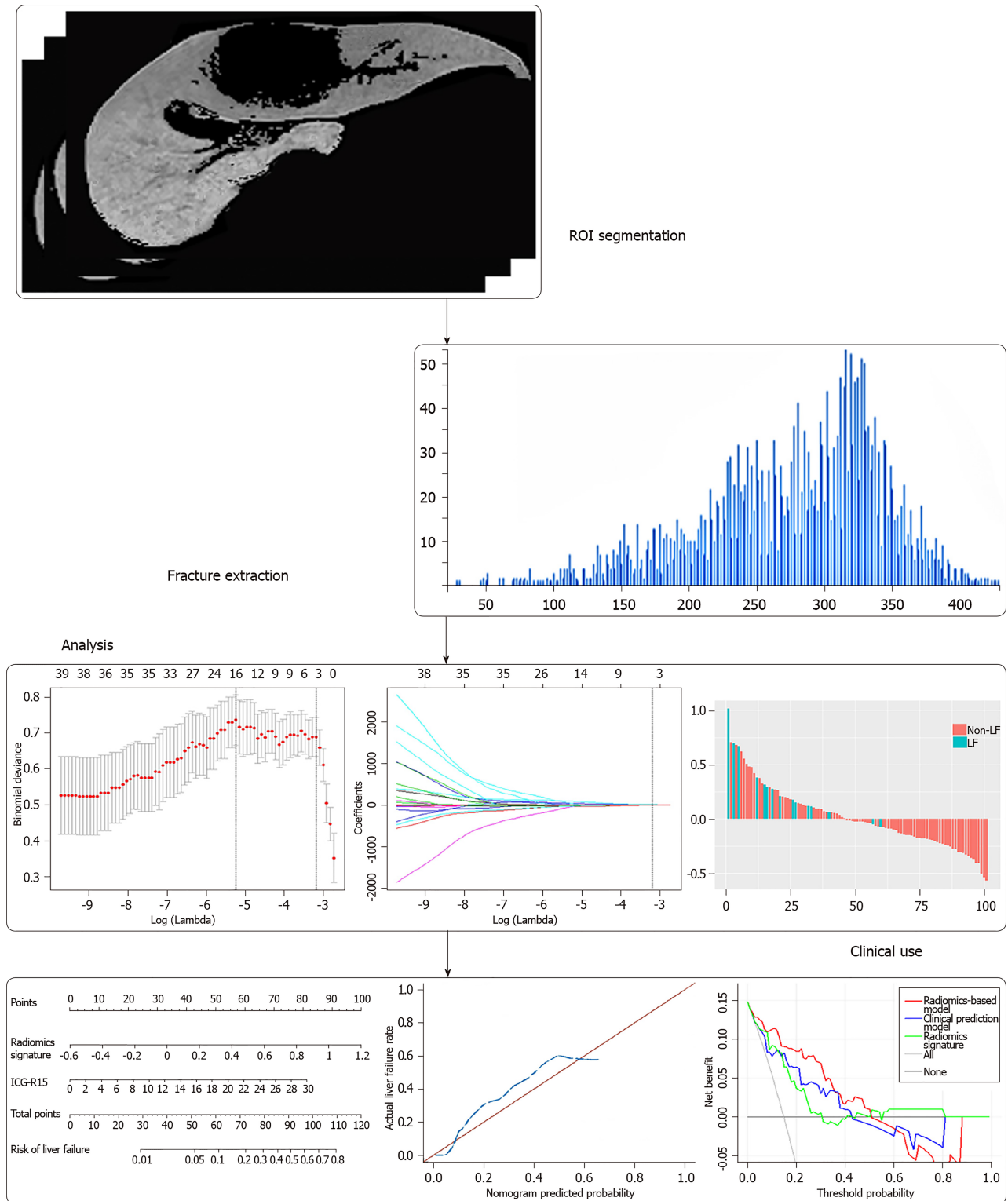


Figure 2 Workflow of necessary steps in current study. Region of interests were drawn on hepatobiliary phase gadoteric acid-enhanced magnetic resonance images. For feature selection, the least absolute shrinkage and selection operator method was applied to select significant features. The radiomics signature was constructed by a linear combination of selected features. The performance of the prediction model was assessed by the area under a receiver operating characteristic curve and the calibration curve. To provide a more understandable outcome measure, a nomogram was built for individualized evaluation, followed by decision curve analysis. ROIs: Region of interests.

selected by LASSO regression analysis (Figure 3), including minimum intensity (first-order), uniformity (first-order), energy (first-order), cluster prominence (GLCM), and minimum intensity (GLCM). The radiomics signature was constructed by the calculation of radiomics score of these five features according to the following formula:

$$\text{Radiomics scores} = -4.712031 - 1.529694 \times 10^{-4} \times \text{minimum intensity} + 5.788767 \times$$

Table 2 Clinicopathological characteristics of 101 hepatitis B virus-related cirrhotic patients with hepatocellular carcinoma

	Patients with Liver failure, <i>n</i> = 15	Patients without Liver failure, <i>n</i> = 86	<i>P</i> value
Sex			0.439
Male	9 (90)	50 (89)	
Female	1 (10)	6 (12)	
Age in yr	55 (22-78)	55 (40-67)	0.958
Primary tumor			
Tumor size in mm ¹²	59 (15-154)	38 (10-197)	0.069
Single, <i>n</i>	4 (27)	60 (70)	
Multiple in <i>n</i>	11 (73)	26 (30)	
Baseline serological index ¹			
Aspartate aminotransferase in IU/L	59 (17-116)	33 (17-1663)	0.030
Alanine aminotransferase in IU/L	34 (17-98)	31 (11-1491)	0.248
Total bilirubin in mg/dL	18.2 (8.2-37.9)	15.7 (3.2-35.5)	0.314
Albumin in g/L	38.7 (30.9-45.8)	40.3 (23.0-50.3)	0.135
Alkaline phosphatase in U/L	131 (71-365)	91 (41-410)	0.004
Platelet as /L	200 (111-496)	188 (49-489)	0.462
Prothrombin time in s	12.8 (11.3-14.9)	12.3 (10.6-16.8)	0.138
Cholinesterase in U/L	6271 (2522-8417)	6714 (2334-12360)	0.110
ICG test ¹			
Elimination rate constant in K as min ⁻¹	0.13 (0.09-0.19)	0.21 (0.12-0.29)	0.308
Retention rate at 15 min as R15 in %	8.2 (1.3-28.4)	12.8 (6.1-18.0)	0.002
The half-life as T1/2 in min	6.36 (3.73-7.88)	3.27 (2.39-5.68)	0.061
Baseline score			
Child-Pugh classification			0.786
A	15 (100)	81 (94)	
B	0 (0)	5 (6)	
C	0 (0)	0 (0)	
Fibrosis grade on specimen			0.174
F1	1 (7)	9 (11)	
F2	0 (0)	8 (9)	
F3	0 (0)	7 (8)	
F4	9 (60)	14 (16)	
N/A	5 (33)	48 (56)	

Data are numbers of patients, with percentages in parentheses, except otherwise indicated.

¹Numbers in parentheses are ranges;

²If the number of lesions is greater than 2, the largest lesion was chosen to measure the maximal dimension.

N/A: Not available.

uniformity + 7.658610×energy - 3.20757210⁻⁹×cluster prominence(GLCM) - 1.566187×10⁻⁶ × minimum intensity (GLCM).

Development of radiomics-based prediction model

The significant clinical variables including ALP level and ICG-R15, and radiomics signature were chosen to build the radiomics-based model. The collinearity diagnosis showed the variance inflation factors of ALP, ICG-R15 and radiomics signature ranging from 1.012 to 1.107, suggesting no multicollinearity for radiomics-based model. Multivariable logistic regression analysis showed that only ICG-R15 and radiomics signature were independent risk factors for liver failure ($P < 0.005$). Thus, the radiomics signature and ICG-R15 were incorporated to develop the radiomics-based model and presented as a nomogram (Figure 4A). The calibration curve and an insignificant Hosmer-Lemeshow test statistic ($P = 0.841$) demonstrated the good calibration of this nomogram (Figure 4C).

Comparison of predictive performance

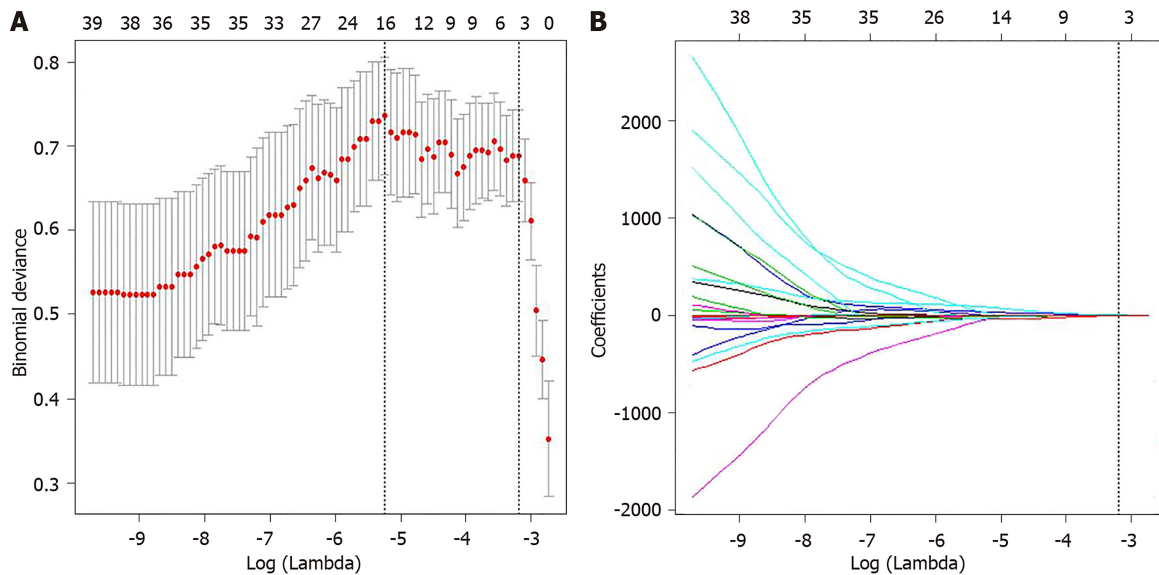


Figure 3 Radiomic feature selection using least absolute shrinkage and selection operator logistic regression. A: Selection of tuning parameters (λ) in the least absolute shrinkage and selection operator model used 10-fold cross-validation via minimum criteria. The area under the curve was plotted vs $\log(\lambda)$. Dotted vertical lines were drawn at the optimal values using the minimum criteria and the 1 standard error of the minimum criteria (the 1 - standard error criteria); B: Least absolute shrinkage and selection operator coefficient profiles of the radiomic features. A vertical line was plotted at the optimal λ value, which resulted in five features with nonzero coefficients.

The predictive performance of clinical prediction model, radiomics signature, and radiomics-based model is shown in Table 3 and the ROCs are shown in Figure 4B. The radiomics-based model showed the highest performance for predicting liver failure, with an AUC of 0.894 (95%CI: 0.823, 0.964), which was higher than that of the clinical prediction model [AUC, 0.810 (95%CI: 0.691, 0.929)] and radiomics signature [AUC, 0.809 (95%CI: 0.713, 0.906)] ($P = 0.025$). The IDI showed a significant improvement in the accuracy of predicting liver failure when radiomics signature was incorporated with the clinical prediction model (IDI = 0.117, $P = 0.002$; continuous net reclassification improvement = 0.157, $P = 0.09$). The decision curve analysis for clinical prediction model, radiomics signature and radiomics-based model are presented in Figure 5.

DISCUSSION

Our study demonstrated that several radiomic features derived from HBP images of gadoteric acid-enhanced MRI are associated with the liver failure in cirrhotic patients with HCC after major hepatectomy. Radiomics signature constructed from these radiomic features showed good performance in predicting postoperative liver failure. Radiomics-based model integrating radiomics signature and ICG-R15 further improved the predictive performance.

For hepatitis B patients with active viral replication, liver disease like cirrhosis not only can progress to the stage of liver function decompensation, but also can result in the occurrence of HCC^[20]. As surgery is the primary treatment for patients with HCC, it is important to assess liver functional reserve for HCC patients before surgery. At present, the main clinical factors that could help predict the risk of postoperative liver failure are serological indexes, Child-Pugh classification or IGG test. An increased ALP activity often accompanies hepatobiliary disease^[21]. Previously, the ALP level was found to be useful for estimating postoperative liver failure after hepatectomy^[22]. Another study showed that serum ALP and bilirubin might be an early surrogate marker for ischemic cholangiopathy and graft failure in liver transplantation^[23]. In our study, the ALP level was also found to be an independent predictor of liver failure. Unlike a single serological index, Child-Pugh classification incorporates several biochemical parameters and clinical symptoms, suggesting insufficient liver function. However, the Child-Pugh classification has been proven not reliable for predicting the prognosis of hepatectomy due to its high variability^[24,25]. In our study, Child-Pugh classification was not associated with the occurrence of liver failure.

The ICG clearance test is another important method to evaluate liver function, which is commonly used in clinical daily practice^[26]. The results of the ICG test are

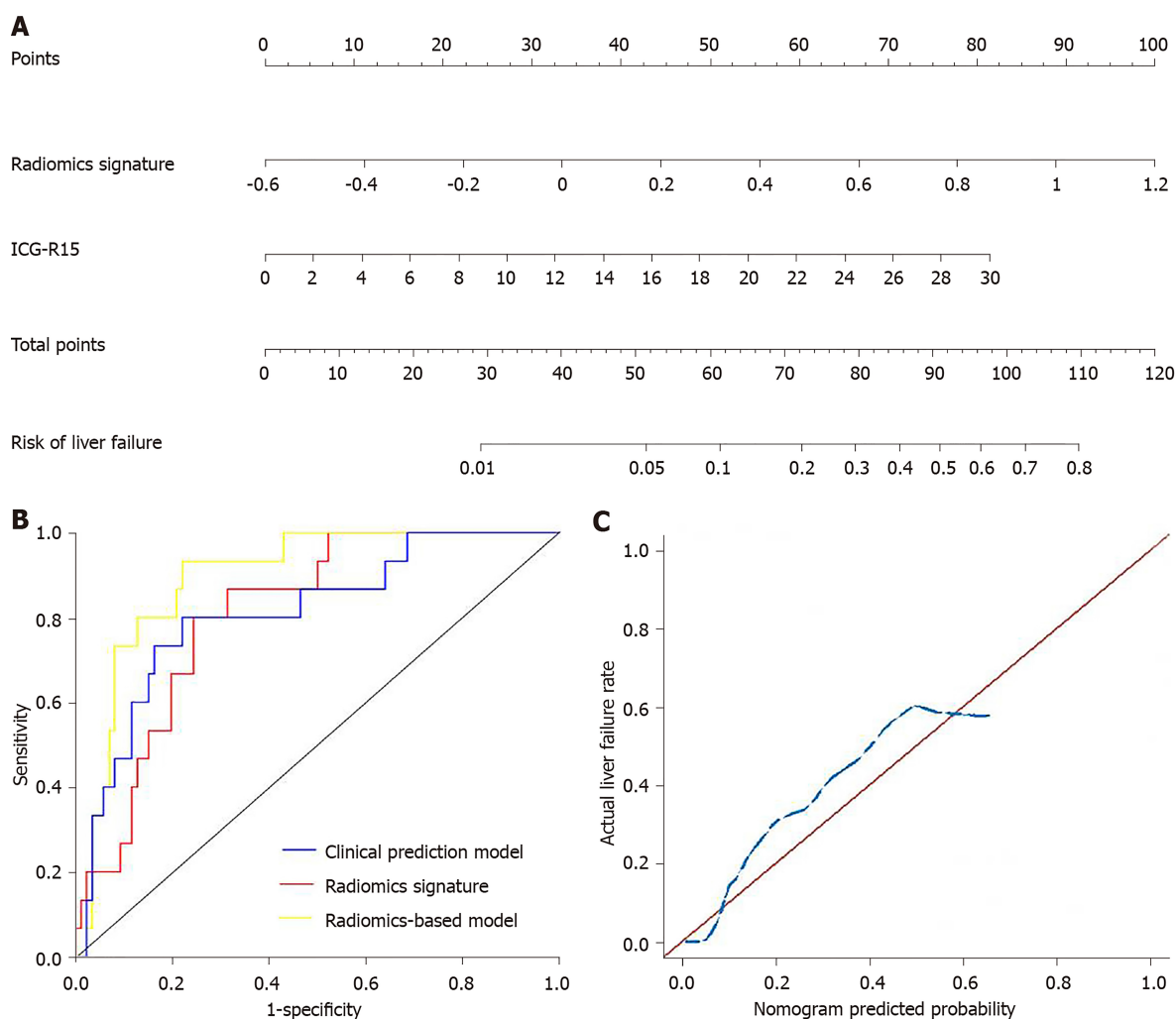


Figure 4 Radiomics nomogram and receiver operating characteristic curves and calibration curves of three predictive models. A: A nomogram was developed with incorporation of radiomics signature and indocyanine green retention rate at 15 min; B: Comparison of receiver operating characteristic curves of clinical prediction model, radiomics signature and radiomics-based model for the prediction of liver failure; C: Calibration curves of the nomogram.

considered as the most reliable risk factor, which can be used to determine the surgical indications of patients with HCC^[27]. However, the ICG test has several limitations. For example, this test cannot be used in patients with jaundice. Moreover, a previous study showed that the predictive value of the ICG test for LF was nearly equal to a random guess (AUC, 0.51)^[28]. In our study, 6 patients with a normal ICG-R15 value have experienced liver failure after surgery.

Several imaging biomarkers, such as liver volume measured on three-dimensional CT, receptor index (LHL₁₅) and blood clearance index (HH₁₅) on ^{99m}Tc-galactosyl serum albumin scintigraphy, have been applied to assess liver function^[29]. However, the liver volume is not always relevant to the actual liver function, and the heterogeneity of the remnant liver may result in different levels of function for two patients with the same remnant liver volume on CT. The disadvantages of ^{99m}Tc-galactosyl serum albumin scintigraphy are the radiation exposure and its low spatial resolution. Gadoxetic acid-enhanced MRI has a high diagnostic efficacy for focal hepatic lesions^[30] and can be used to quantify liver function^[8]. The liver in patients with hepatitis B shows slow-moving changes with a common pathological process of progressive fibrosis, bridging of portal spaces and nodule regeneration of the liver parenchyma^[31]. Liver damage may result in decreased number of normal hepatocytes, which impairs the uptake of gadoxetic acid, thus lowering the concentrations of gadoxetic acid in the liver parenchyma in the HBP. Moreover, such pathological process that may destroy the homogeneity of the liver parenchyma, which can be reflected by different texture features derived from MRI^[32].

In our study, a radiomics signature based on HBP images was developed for predicting liver failure in patients with HCC. The AUC of radiomics signature was as high as 0.809, which suggests favorable discrimination for liver failure. The multivariable logistic regression analysis showed that ALP and ICG-R15 were

Table 3 Receiver operating characteristics analysis of the predictive value of clinical prediction model, radiomics signature and radiomics-based model

	Clinical prediction model	Radiomics signature	Radiomics-based model
AUC (95%CI)	0.810 (0.691-0.929)	0.809 (0.713-0.906)	0.894 (0.823-0.964)
Optimized Youden Index	0.579	0.556	0.712
Sensitivity (95%CI)	0.800 (0.514-0.947)	0.800 (0.514-0.947)	0.933 (0.660-0.997)
Specificity (95%CI)	0.779 (0.674-0.858)	0.756 (0.649-0.839)	0.779 (0.674-0.859)
PPV (95%CI)	0.387 (0.224-0.577)	0.364 (0.210-0.549)	0.424 (0.260-0.606)
NPV (95%CI)	0.957 (0.872-0.989)	0.956 (0.868-0.989)	0.985 (0.910-0.999)
Accuracy (95%CI)	0.782 (0.691-0.852)	0.762 (0.670-0.835)	0.802 (0.713-0.869)

AUC: Area under the curve; CI: Confidence interval; NPV: Negative predictive value; PPV: Positive predictive value.

independent clinical predictive factors for the liver failure. Then, we constructed a radiomics nomogram incorporating the clinical predictive factors and radiomics signature. Only were ICG-R15 and radiomics signature selected as independent predictive factors for the liver failure. This radiomics-based model showed good calibration and discrimination. The AUC of the nomogram increased to 0.894, and the IDI index has the significance, indicating the greater predictive efficacy of nomogram than either the radiomics signature or the clinical variables alone. Previously, several texture features derived from preoperative CT images has also been proposed to predict postoperative liver failure^[16]. However, this study has a small number of patients ($n = 36$) and no predictive model was built^[16]. In addition, the measurement of relative liver enhancement on HBP images of gadoxetic acid-enhanced magnetic resonance imaging (MRI) has been shown to be able to preoperatively assess the risk of liver failure after major liver resection with an AUC of 0.948^[9]. However, only a small number of patients with liver failure ($n = 3$) was included in this study. The value of relative liver enhancement should be further validated by a large cohort study.

Gadoxetic acid-enhanced MRI can assist in differential diagnosis of focal liver lesion. The radiomics model built from HBP images has an advantage to be used for preoperative liver function assessment in the same examination. The proposed radiomics-based model in our study may serve as a reliable predictive tool to reduce postoperatively liver failure and mortality in cirrhotic patients with HCC after major hepatectomy. For example, it can be used in combination with ICG-R15 to improve the ability to predict postoperative liver failure when surgery is planned for a cirrhotic patient with HCC. If there is a high risk of postoperative liver failure, major hepatectomy should be avoided and some locoregional treatments such as percutaneous ethanol injection, radiofrequency ablation, trans-arterial chemoembolization and radioembolization can be applied for this patient. In addition, if a patient has uncertain results of ICG test, such as a patient with severe jaundice, the radiomics model can be used alternatively to predict the risk of postoperative live failure^[33].

Our study had several limitations. First, a small number of patients with liver failure in our study, thus the validation cohort can't be allocated. After all, liver failure is a relatively rare event in our institution due to strict selection for hepatectomy. Second, we did not adopt a large quantity of radiomic features, since most of the information from feature exaction were redundant and nonreproducible^[34].

In conclusion, a radiomics signature based on preoperative gadoxetic acid-enhanced MRI was developed, which showed favorable performance in predicting liver failure in cirrhotic patients with HCC after major liver resection. The radiomics model incorporating the radiomics signature and ICG-15 further improved the performance in predicting liver failure. The radiomics analysis of preoperative gadoxetic acid-enhanced MRI could be used to predict the risk of liver failure in cirrhotic patients with HCC after major hepatectomy.

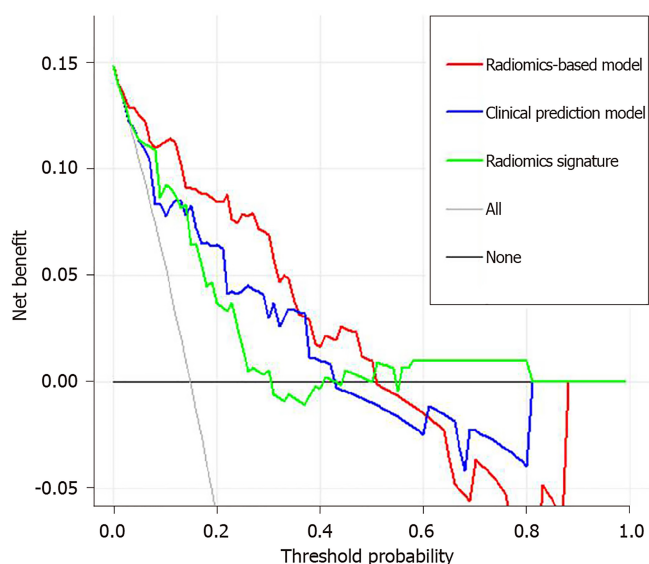


Figure 5 Decision curve analysis for each model. The y-axis measures the net benefit, which is calculated by summing the benefits (true-positive findings) and subtracting the harms (false-positive findings), weighting the latter by a factor related to the relative harm of undetected liver failure compared with the harm of unnecessary treatment. The decision curve showed the application of radiomics-based model to predict liver failure adds more benefit than treating all or none of the patients, clinical prediction model, and radiomics signature.

ARTICLE HIGHLIGHTS

Research background

Postoperative liver failure is the most serious complication for patients with hepatocellular carcinoma (HCC) after major hepatectomy. There are many methods for predicting postoperative liver failure after hepatectomy but not sufficiently accurate enough. This paper provides a radiomics model based on gadoxetic acid-enhanced magnetic resonance imaging (MRI), serve as a reliable predictive tool to reduce postoperative liver failure and mortality in cirrhotic patients with HCC after major hepatectomy.

Research motivation

In order to determine a new method to predict the postoperative liver failure after major hepatectomy and our radiomics model showed a favorable performance. However, the results obtained in this study need to be further verified in the population, and validation cohort need to be allocated.

Research objectives

The objective of this study is to determine the performance for predicting liver failure of a radiomics model based on preoperative gadoxetic acid-enhanced magnetic resonance imaging. The finding provides important information for medical decision making when surgery is required for a patient with HCC.

Research methods

The significant clinical variables were chosen and the radiomics signature was developed based on preoperative hepatobiliary phase gadoxetic acid-enhanced MRI in 101 patients with HCC from Sun Yat-Sen Memorial Hospital. The integrated radiomics-based model was presented as a radiomics nomogram. The performances for predicting post-operative liver failure were determined using receiver operating characteristics curve, calibration curve and decision curve analysis.

Research results

This study found that five radiomic features from hepatobiliary phase images were selected, and a radiomics-based model incorporating indocyanine green clearance rate at 15 min and radiomics signature showed favorable performance for predicting postoperative liver failure. The performance of radiomics model need to be further validated.

Research conclusions

The liver failure is very severe after liver resection. In this study, a radiomics signature based on preoperative gadoxetic acid-enhanced MRI was developed, which showed favorable performance in predicting liver failure in cirrhotic patients with HCC after major liver resection.

Research perspectives

This study confirmed the performance for predicting of our radiomics model. On this basis, future studies will further expand the sample size, and add the validation cohort.

REFERENCES

- 1 **Lock JF**, Reinhold T, Malinowski M, Pratschke J, Neuhaus P, Stockmann M. The costs of postoperative liver failure and the economic impact of liver function capacity after extended liver resection--a single-center experience. *Langenbecks Arch Surg* 2009; **394**: 1047-1056 [PMID: [19533168](#) DOI: [10.1007/s00423-009-0518-4](#)]
- 2 **Zipprich A**, Kuss O, Rogowski S, Kleber G, Lotterer E, Seufferlein T, Fleig WE, Dollinger MM. Incorporating indocyanin green clearance into the Model for End Stage Liver Disease (MELD-ICG) improves prognostic accuracy in intermediate to advanced cirrhosis. *Gut* 2010; **59**: 963-968 [PMID: [20581243](#) DOI: [10.1136/gut.2010.208595](#)]
- 3 **Zappa M**, Dondero F, Sibert A, Vullierme MP, Belghiti J, Vilgrain V. Liver regeneration at day 7 after right hepatectomy: global and segmental volumetric analysis by using CT. *Radiology* 2009; **252**: 426-432 [PMID: [19703882](#) DOI: [10.1148/radiol.2522080922](#)]
- 4 **Cucchetti A**, Ercolani G, Vivarelli M, Cescon M, Ravaioli M, La Barba G, Zanello M, Grazi GL, Pinna AD. Impact of model for end-stage liver disease (MELD) score on prognosis after hepatectomy for hepatocellular carcinoma on cirrhosis. *Liver Transpl* 2006; **12**: 966-971 [PMID: [16598792](#) DOI: [10.1002/lt.20761](#)]
- 5 **Kamath PS**, Kim WR; Advanced Liver Disease Study Group. The model for end-stage liver disease (MELD). *Hepatology* 2007; **45**: 797-805 [PMID: [17326206](#) DOI: [10.1002/hep.21563](#)]
- 6 **Hoekstra LT**, de Graaf W, Nibourg GA, Heger M, Bennink RJ, Stieger B, van Gulik TM. Physiological and biochemical basis of clinical liver function tests: a review. *Ann Surg* 2013; **257**: 27-36 [PMID: [22836216](#) DOI: [10.1097/SLA.0b013e31825d5d47](#)]
- 7 **Lee NK**, Kim S, Lee JW, Lee SH, Kang DH, Kim GH, Seo HI. Biliary MR imaging with Gd-EOB-DTPA and its clinical applications. *Radiographics* 2009; **29**: 1707-1724 [PMID: [19959517](#) DOI: [10.1148/rg.296095501](#)]
- 8 **Yamada A**, Hara T, Li F, Fujinaga Y, Ueda K, Kadoya M, Doi K. Quantitative evaluation of liver function with use of gadoxetate disodium-enhanced MR imaging. *Radiology* 2011; **260**: 727-733 [PMID: [21712472](#) DOI: [10.1148/radiol.11100586](#)]
- 9 **Wibmer A**, Prusa AM, Nolz R, Gruenberger T, Schindl M, Ba-Ssalamah A. Liver failure after major liver resection: risk assessment by using preoperative Gadoteric acid-enhanced 3-T MR imaging. *Radiology* 2013; **269**: 777-786 [PMID: [23942606](#) DOI: [10.1148/radiol.13130210](#)]
- 10 **Ratzl V**, Charlotte F, Heurtier A, Gombert S, Giral P, Bruckert E, Grimaldi A, Capron F, Poynard T; LIDO Study Group. Sampling variability of liver biopsy in nonalcoholic fatty liver disease. *Gastroenterology* 2005; **128**: 1898-1906 [PMID: [15940625](#) DOI: [10.1053/j.gastro.2005.03.084](#)]
- 11 **Yoon JH**, Choi JI, Jeong YY, Schenk A, Chen L, Laue H, Kim SY, Lee JM. Pre-treatment estimation of future remnant liver function using gadoteric acid MRI in patients with HCC. *J Hepatol* 2016; **65**: 1155-1162 [PMID: [27476767](#) DOI: [10.1016/j.jhep.2016.07.024](#)]
- 12 **Lambin P**, Leijenaar RTH, Deist TM, Peerlings J, de Jong EEC, van Timmeren J, Sanduleanu S, Larue RTHM, Even AJG, Jochems A, van Wijk Y, Woodruff H, van Soest J, Lustberg T, Roelofs E, van Elmpst W, Dekker A, Mottaghy FM, Wildberger JE, Walsh S. Radiomics: the bridge between medical imaging and personalized medicine. *Nat Rev Clin Oncol* 2017; **14**: 749-762 [PMID: [28975929](#) DOI: [10.1038/nrclinonc.2017.141](#)]
- 13 **Limkin EJ**, Sun R, Dercle L, Zacharakis EI, Robert C, Reuzé S, Schernberg A, Paragios N, Deutsch E, Ferti C. Promises and challenges for the implementation of computational medical imaging (radiomics) in oncology. *Ann Oncol* 2017; **28**: 1191-1206 [PMID: [28168275](#) DOI: [10.1093/annonc/mdx034](#)]
- 14 **Ji GW**, Zhang YD, Zhang H, Zhu FP, Wang K, Xia YX, Zhang YD, Jiang WJ, Li XC, Wang XH. Biliary Tract Cancer at CT: A Radiomics-based Model to Predict Lymph Node Metastasis and Survival Outcomes. *Radiology* 2019; **290**: 90-98 [PMID: [30325283](#) DOI: [10.1148/radiol.2018181408](#)]
- 15 **Wu S**, Zheng J, Li Y, Yu H, Shi S, Xie W, Liu H, Su Y, Huang J, Lin T. A Radiomics Nomogram for the Preoperative Prediction of Lymph Node Metastasis in Bladder Cancer. *Clin Cancer Res* 2017; **23**: 6904-6911 [PMID: [28874414](#) DOI: [10.1158/1078-0432.CCR-17-1510](#)]
- 16 **Simpson AL**, Adams LB, Allen PJ, D'Angelica MI, DeMatteo RP, Fong Y, Kingham TP, Leung U, Miga MI, Parada EP, Jarnagin WR, Do RK. Texture analysis of preoperative CT images for prediction of postoperative hepatic insufficiency: a preliminary study. *J Am Coll Surg* 2015; **220**: 339-346 [PMID: [25537305](#) DOI: [10.1016/j.jamcollsurg.2014.11.027](#)]
- 17 **Krieger PM**, Tamandl D, Herberger B, Faybik P, Fleischmann E, Maresch J, Gruenberger T. Evaluation of chemotherapy-associated liver injury in patients with colorectal cancer liver metastases using indocyanine green clearance testing. *Ann Surg Oncol* 2011; **18**: 1644-1650 [PMID: [21207168](#) DOI: [10.1245/s10434-010-1494-1](#)]
- 18 **Shiha G**, Zalata K. Ishak versus METAVIR: terminology, convertibility and correlation with laboratory changes in chronic Hepatitis C. *InTechOpen*. 2011; 156-170 [DOI: [10.5772/20110](#)]
- 19 **Tibshirani R**. Regression shrinkage and selection via the lasso. *J R Stat Soc Series B Stat Methodol* 1996; **58**: 267-88
- 20 **Peng CY**, Chien RN, Liaw YF. Hepatitis B virus-related decompensated liver cirrhosis: benefits of antiviral therapy. *J Hepatol* 2012; **57**: 442-450 [PMID: [22504333](#) DOI: [10.1016/j.jhep.2012.02.033](#)]
- 21 **Moss DW**. Alkaline phosphatase isoenzymes. *Clin Chem* 1982; **28**: 2007-2016 [PMID: [6751596](#) DOI: [10.1093/clinchem/28.10.2007](#)]
- 22 **Osada S**, Saji S. The clinical significance of monitoring alkaline phosphatase level to estimate postoperative liver failure after hepatectomy. *Hepatogastroenterology* 2004; **51**: 1434-1438 [PMID: [15362770](#) DOI: [10.1002/hed.20094](#)]
- 23 **Halldorson JB**, Rayhill S, Bakthavatsalam R, Montenegro M, Dick A, Perkins J, Reyes J. Serum alkaline phosphatase and bilirubin are early surrogate markers for ischemic cholangiopathy and graft failure in liver transplantation from donation after circulatory death. *Transplant Proc* 2015; **47**: 465-468 [PMID: [25769592](#) DOI: [10.1016/j.transproceed.2014.10.055](#)]
- 24 **Nagashima I**, Takada T, Okinaga K, Nagawa H. A scoring system for the assessment of the risk of mortality after partial hepatectomy in patients with chronic liver dysfunction. *J Hepatobiliary Pancreat Surg* 2005; **12**: 44-48 [PMID: [15754099](#) DOI: [10.1007/s00534-004-0953-0](#)]
- 25 **Garcea G**, Ong SL, Maddern GJ. Predicting liver failure following major hepatectomy. *Dig Liver Dis* 2009; **41**: 798-806 [PMID: [19303376](#) DOI: [10.1016/j.dld.2009.01.015](#)]
- 26 **Matsumata T**, Kanematsu T, Yoshida Y, Furuta T, Yanaga K, Sugimachi K. The indocyanine green test enables prediction of postoperative complications after hepatic resection. *World J Surg* 1987; **11**: 678-681

- [PMID: 2823492 DOI: 10.1007/bf01655848]
- 27 **Ishikawa M**, Yogita S, Miyake H, Fukuda Y, Harada M, Wada D, Tashiro S. Clarification of risk factors for hepatectomy in patients with hepatocellular carcinoma. *Hepatogastroenterology* 2002; **49**: 1625-1631 [PMID: 12397750 DOI: 10.1136/gut.51.5.757]
 - 28 **Wong JS**, Wong GL, Chan AW, Wong VW, Cheung YS, Chong CN, Wong J, Lee KF, Chan HL, Lai PB. Liver stiffness measurement by transient elastography as a predictor on posthepatectomy outcomes. *Ann Surg* 2013; **257**: 922-928 [PMID: 23001077 DOI: 10.1097/SLA.0b013e318269d2ec]
 - 29 **Kawamura H**, Kamiyama T, Nakagawa T, Nakanishi K, Yokoo H, Tahara M, Kamachi H, Toi H, Matsushita M, Todo S. Preoperative evaluation of hepatic functional reserve by converted ICGR15 calculated from Tc-GSA scintigraphy. *J Gastroenterol Hepatol* 2008; **23**: 1235-1241 [PMID: 18522682 DOI: 10.1111/j.1440-1746.2008.05389.x]
 - 30 **Reimer P**, Schneider G, Schima W. Hepatobiliary contrast agents for contrast-enhanced MRI of the liver: properties, clinical development and applications. *Eur Radiol* 2004; **14**: 559-578 [PMID: 14986050 DOI: 10.1007/s00330-004-2236-1]
 - 31 **Tsochatzis EA**, Bosch J, Burroughs AK. Liver cirrhosis. *Lancet* 2014; **383**: 1749-1761 [PMID: 24480518 DOI: 10.1016/S0140-6736(14)60121-5]
 - 32 **Wu Z**, Matsui O, Kitao A, Kozaka K, Koda W, Kobayashi S, Ryu Y, Minami T, Sanada J, Gabata T. Hepatitis C related chronic liver cirrhosis: feasibility of texture analysis of MR images for classification of fibrosis stage and necroinflammatory activity grade. *PLoS One* 2015; **10**: e0118297 [PMID: 25742285 DOI: 10.1371/journal.pone.0118297]
 - 33 **Bruix J**, Sherman M; American Association for the Study of Liver Diseases. Management of hepatocellular carcinoma: an update. *Hepatology* 2011; **53**: 1020-1022 [PMID: 21374666 DOI: 10.1002/hep.24199]
 - 34 **Berenguer R**, Pastor-Juan MDR, Canales-Vázquez J, Castro-García M, Villas MV, Mansilla Legorburo F, Sabater S. Radiomics of CT Features May Be Nonreproducible and Redundant: Influence of CT Acquisition Parameters. *Radiology* 2018; **288**: 407-415 [PMID: 29688159 DOI: 10.1148/radiol.2018172361]



Published By Baishideng Publishing Group Inc
7041 Koll Center Parkway, Suite 160, Pleasanton, CA 94566, USA
Telephone: +1-925-3991568
E-mail: bpgoffice@wjgnet.com
Help Desk: <http://www.f6publishing.com/helpdesk>
<http://www.wjgnet.com>

